Contents list available at CBIORE journal website

International Journal of Renewable Energy Development

Journal homepage: https://ijred.cbiore.id

Research Article

Data-driven reconstruction of solar spectrum in a class A+ LED solar simulator

Khanittha Wannakam[a], Chaiyant Boonmee[a], Kreeta Sukthang[b*], Saichol Chudjuarjeen[c], Wattanawong Romsai[d], Napat Watjanatepin[d]

[a]*Department of Electrical Engineering, Faculty of Engineering and Architecture, Rajamangala University of Technology Suvarnabhumi, Nonthaburi, Thailand*

[b] *Department of Mechatronics Engineering, Faculty of Engineering and Architecture, Rajamangala University of Technology Suvarnabhumi, Nonthaburi, Thailand*

[c] *Department of Electrical Engineering, Faculty of Engineering, Rajamangala University of Technology Krungthep, Bangkok, Thailand*

[d] *Department of Electrical Engineering, Faculty of Engineering, Bangkokthonburi University, Bangkok, Thailand*

Abstract. High-spectral-fidelity solar simulators are indispensable for rigorous photovoltaic characterization, as they provide stable, reproducible irradiance that closely conforms to the AM 1.5G reference spectrum. The latest IEC 60904-9:2020 standard imposes stringent limits on spectral mismatch (SM), coverage, and deviation, driving the need for innovative design strategies. This work introduces a data-driven LED spectrum reconstruction methodology to engineer a Class A+ LED Solar Simulator (LSS) spectrum. Manufacturer-provided spectral profiles spanning 300–1200 nm were digitized using a precision plot-digitization tool and calibrated via a Spectral Mismatch Calculator to ensure wavelength alignment and intensity normalization. Custom numerical optimization algorithms then refined these datasets to compute the optimal mixing ratios of broadband phosphor-converted white LEDs (400–900 nm), combined with targeted UV, visible, and NIR emitters. The finalized 13-LED configuration achieved a Spectral Coverage (SPC) of 99.52% and a Spectral Deviation (SPD) of 17.42%, exceeding the Class A+ acceptance criteria while employing a minimal component count. Although minor uncertainties may originate from the digitization process, such as image resolution and axis calibration, these can be effectively mitigated by integrating direct numerical spectra supplied by manufacturers. This approach establishes an efficient, high-accuracy framework for LSS spectral design. Future work will advance to hardware prototyping and empirical validation of the simulator's irradiance spectrum under real-world operating conditions, fully compliant with IEC 60904-9:2020.

Keywords: Data-Driven Reconstruction, LED Solar Simulator, Spectral Coverage, Spectral Deviation, LED Spectral Data

Received: 22nd June 2025; Revised: 17th August 2025; Accepted: 6th Sept 2025; Available online: 10th Sept 2025

1. Introduction

Light Emitting Diodes (LEDs) are a transformative innovation that has revolutionized the lighting industry, shifting from traditional incandescent bulbs to solid-state lighting (Islam *et al.* 2021). LEDs offer high efficiency (Sena *et al.* 2024), energy savings (Katzin *et al.* 2021), easy adjustment of color and brightness (Hasan *et al.* 2024), and digitally controllable light emission (Ge *et al.* 2021). Additionally, they possess significantly longer lifespans than conventional light sources (Watjanatepin *et al.* 2023). In photovoltaic research, LED-based solar simulators (LSS) demonstrate clear advantages over traditional Xenon arc lamps (Leary *et al.* 2016). These advantages include the elimination of optical components such as lenses and spectrum filters (Chojniak *et al.* 2024), precise spectral tunability (Sevilla-Camacho *et al.* 2024), reduced thermal load (Parupudi, *et al.* 2019), and improved operational stability (Esen *et al.* 2017).

A solar simulator is a device designed to replicate the spectral distribution and intensity of sunlight at the Earth's surface (Cortés-Severino *et al.* 2021). It is used as a standardized light source for testing the performance of solar cells (King *et al.* 2023), or other photosensitive materials (Yang *et al.* 2025), providing a reliable alternative to natural sunlight (Sun *et al.* 2023), which is subject to weather variability and spectral inconsistency. To accurately mimic the solar spectrum at ground level, LSSs must generate a radiation profile with minimal deviation from the AM 1.5G standard (Basore *et al.* 2021). The spectrum must cover the wavelength range of 300 nm to 1200 nm and meet the performance criteria for Class A+ solar simulators spectrum. Moreover, the spectrum should achieve optimal values of SPD and SPC (Vosylius *et al.* 2023), in compliance with the IEC 60904-9:2020 standard (International Electrotechnical Commission. 2020), to ensure minimal errors in solar cell testing.

Although LED manufacturers provide a wide range of SPD graphs, most of these LEDs do not adequately cover the wavelength range required for solar simulator applications. Additionally, the available data typically comes in two formats: numerical spectral data and graphical representations, the latter of which is difficult to use directly. Moreover, combining multiple LED types to match the AM 1.5G spectrum within the strict tolerance limits required for Class A+ performance under the latest standard (International Electrotechnical Commission. 2020) often necessitates the use of a large number of LED types.

*Corresponding author
Email: kreeta.s@rmutsb.ac.th (K. Sukthang)

https://doi.org/10.61435/ijred.2025.61502
ISSN: 2252-4940/© 2025.The Author(s). Published by CBIORE

Previous studies (Watjanatepin *et al.* 2023, Sun *et al.* 2022, Al-Ahmad *et al.* 2022, Tavakoli *et al.* 2021, López-Fraguas *et al.* 2019, Linden *et al.* 2014, Cruz *et al.* 2025, Song *et al.* 2021) have reported using between 6 and 23 different LED types. Therefore, meticulous numerical spectrum synthesis is essential to construct an accurate target spectrum. Without access to high-resolution spectral data and a precise reconstruction algorithm, spectral deviation may occur, reducing solar cell performance testing accuracy. Additionally, covering the full wavelength range of 300 nm to 1200 nm using many LED types increases system complexity, especially in the control architecture, and can lead to non-uniformity in the emitted light.

In this study, the authors utilize broadband phosphor-converted white LEDs (BB-pcWLEDs) based on a single LED chip capable of emitting light across the visible to near-infrared (NIR) range. For instance, in a previous study by the authors (Hou *et al.* 2023), an extra-broadband visible–NIR phosphor-converted LED was developed, covering a wavelength range from 500 to 900 nm. Later, the authors (Zhang *et al.* 2024) presented an ultra-wide visible–NIR pc-LED capable of emitting light from 450 to 900 nm. This aligns with another report by the authors (Wang *et al.* 2023), which introduced multifunctional LEDs composed of pc-WLEDs and pc-NIR LEDs, collectively providing spectral coverage from 400 to 900 nm. These technologies exhibit relatively high color rendering index and are applicable in various fields, including general lighting, industrial vision systems, and food and biotechnology applications (Wang *et al.* 2019, Vosylius *et al.* 2022 & Turek *et al.* 2019).

From another perspective, the authors suggest that BB-pcWLEDs, which emit a broad output spectrum covering the visible to NIR range, can serve as effective light sources for solar simulators. Due to their wide spectral coverage typically from 400 to 900 nm BB-pcWLEDs can significantly reduce the number of LED types required to synthesize light within this wavelength range. Therefore, by supplementing the spectrum of BB-pcWLEDs with that of selected UV-NIR and visible LEDs, it is possible to achieve the required spectral range as specified by the IEC 60904-9:2020 standard, while also allowing flexible adjustment of the intensity of each LED channel. This raises two key research questions: (1) To what extent, and in what way, can the use of BB-pcWLEDs reduce the number of LED types required for a Class A+ LED-based solar simulator? and (2) What approach will yield the best SPC and SPD values?

In this study, we present a method for simulating of the spectrum of an LSS using a Data-Driven LED Spectrum Reconstruction approach. The methodology involves: (1) utilizing spectral data from LED manufacturers as input, (2) applying numerical techniques to extract and refine the data, and (3) determining the optimal mixing ratios of different LED channels to emulate the AM 1.5G spectrum within Class A+ spectral mismatch criteria. The objective of this research is to design and simulate the spectrum of an LSS that meets Class A+ standards by employing broadband phosphor-converted white LEDs through a data-driven reconstruction method. The analysis focuses on identifying the minimal number and types of LEDs required to achieve the best possible SPC and SPD. The results yield a high-accuracy irradiance profile and an optimized LED mixing strategy, enabling the design and calibration of an LSS under IEC 60904-9:2020 standards. However, the ASTM E927-10 (Standard Specification for Solar Simulation for Photovoltaic Testing) was not adopted in this study, as its specifications do not align with the primary research objective namely, simulating the spectrum range from 300 to 1200 nm and analyzing the corresponding SPD and SPC parameters. This work lays the groundwork for the development of a physical prototype in future research.

2. Materials and Methods

2.1 Spectrum data of LED

The spectrum data or spectrum profiles of the LEDs used in this study were analyzed based on information from multiple manufacturers. A total of 13 LED types were selected from four manufacturers. These include BB-pcWLEDs, referred to as Hyperspectral LEDs, from EFFILUX, France (EFFILUX. 2025), as well as UV and NIR LEDs from Thorlabs (New Jersey, United States) (Thorlabs Inc. 2025). In addition, NIR LEDs were obtained from EPIGAP OSA Photonics, Germany [16], and Marubeni Corporation, USA (Marubeni America Corporation. 2025). The specifications are summarized in Table 1.

2.2 Data-Driven LED Spectrum Reconstruction

The procedure followed in this study is illustrated in Figure 1 and consists of the following sequential steps: (1) Spectral graphs provided by LED manufacturers were used as the input

Table 1
Details of the LEDs analyzed for their spectral profiles in this study

Spectrum Range	LED types	Model	Manufacture
UV	325nm	M325D3	THORLABS
	340nm	M340D4	
	365nm	M365D2	
	385nm	M385D2	
Vis to NIR	BB-pcWLED 400 to 900 nm	EFFI-FLEX-HSI	EFFILUX
Visible	415nm	M415D2	THORLABS
	470nm	M470D4	
	490nm	M490D3	
	660nm	M660D2	
NIR	880nm	M880D2	EPIGAP OSA
	1000nm	OCI-330-1020P-X-TU	
	1100nm	OCI-490-20 ID1100-XE	
	1150nm	SMT1150D	Marubeni

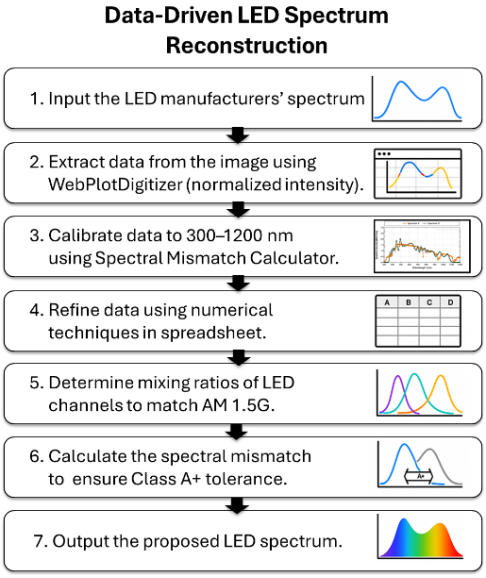

Fig. 1 Data-Driven solar simulator spectrum reconstruction process in this study

data. (2) In cases where the spectrum profiles were available only as image files, the data were extracted using a web-based tool called WebPlotDigitizer (Automeris.io. 2025), which generated spectrum data normalized to a relative intensity of 1.0. (3) The extracted spectral data were then calibrated to cover the wavelength range of 300 to 1200 nm using the Spectral Mismatch Calculator (PV Lighthouse. 2025). (4) The calibrated data were processed and refined using numerical techniques implemented in a spreadsheet. (5) The relative mixing ratios of the various LED channels were determined to closely replicate the AM 1.5G reference spectrum. (6) The spectral mismatch was calculated (International Electrotechnical Commission. 2020) to verify compliance with Class A+ tolerance or better. (7) The final simulated output of this process is the proposed LED spectrum.

2.3 Analyze SPC and SPD

SPC and SPD are quality indicators of the solar simulator spectrum introduced in the IEC 60904-9:2020 standard, which expands upon the previous 2007 edition. Both parameters are referenced against the AM1.5G spectrum. AM1.5G-SPC refers to the percentage of the wavelength range from 300 to 1200 nm where the irradiance power of the solar simulator exceeds 10% of the AM1.5G reference spectrum, as defined in IEC 60904-9:2020. It is calculated as the ratio of the area that meets the threshold to the total area of the entire wavelength range, as shown in Equation (1) (International Electrotechnical Commission. 2020). AM1.5G-SPD, on the other hand, refers to the percentage of the total deviation between the irradiance spectrum of the solar simulator and the AM1.5G reference spectrum. It is determined by summing the absolute differences at each wavelength, multiplying by the bandwidth, and dividing by the total energy of the reference spectrum, as described in Equation (2) (International Electrotechnical Commission. 2020).

The ideal SPC is 100%, indicating that the spectrum fully covers the 300 to 1,200 nm wavelength range. The optimal SPD is 0%, meaning there is minimal deviation from the standard spectrum.

$$\mathrm{SPC} = \left(\left(\sum_{E_{SIM}(\lambda) > 0.1 \times E_{AM1.5}(\lambda)} E_{AM1.5}(\lambda) \cdot \Delta\lambda \right) / \left(\sum_{300\ nm}^{1200\ nm} E_{AM1.5}(\lambda) \cdot \Delta\lambda \right) \right) \cdot 100\% \quad (1)$$

$$\mathrm{SPD} = \left(\left(\sum_{300\ nm}^{1200\ nm} |E_{SIM}(\lambda) - E_{AM1.5}(\lambda)| \cdot \Delta\lambda \right) / \left(\sum_{300\ nm}^{1200\ nm} E_{AM1.5}(\lambda) \cdot \Delta\lambda \right) \right) \cdot 100\% \quad (2)$$

3. Results and Discussion

3.1 Optimize the spectral model of the LED solar simulator

The design approach for simulated the LED spectrum of the LSS is guided by the research objective of achieving Class A+ performance at a target irradiance of 836 W/m² within the wavelength range of 300 nm to 1,200 nm (Vosylius *et al.* 2023). The process begins by utilizing the spectrum data of BB-pcWLEDs (covering 400 to 900 nm) (EFFILUX. 2025), obtained through the data-driven method described in Section 2.2. Numerical techniques were then applied to refine and process the data using a spreadsheet environment.

The first step involves the simulation of ①BB-pcWLED, the irradiance spectrum of the BB-pcWLED was scaled to the highest possible level while maintaining the spectral mismatch (SM)

Table 2
Steps in optimizing the spectrum model by adjusting the irradiance power of each LED type used in this study.

UV-Vis-NIR	①BB-pcWLED		②BB-pcWLED+Vis			③BB-pcWLED+Vis+UV			④BB-pcWLED+Vis+UV		
range	nm	W/m²	nm	W/m²		nm	W/m²		nm	W/m²	
Adding UV	no	0.00	no	0.00	0.00	325	8.01	46.77	325	8.01	46.77
	no		no			340	13.09		340	13.09	
	no		no			365	17.21		365	17.21	
	no		no			385	8.45		385	8.45	
Vis to NIR	400-900	655.83	400-900	618.47	618.47	400-900	618.47	618.47	400-900	618.47	618.47
Adding Vis	no	0.00	415	7.06	40.14	415	7.06	40.14	415	7.06	40.14
	no		470	11.83		470	11.83		470	11.83	
	no		490	12.09		490	12.09		490	12.09	
	no		660	9.17		660	9.17		660	9.17	
Adding NIR	no	0.00	no	0.00	0.00	no	0.00	0.00	880	5.49	129.97
	no		no			no			1000	48.47	
	no		no			no			1100	55.27	
	no		no			no			1150	20.75	
Total Irradiance		655.83		658.61	658.61		705.38	705.38		835.36	835.36

Table 3
compares the changes in irradiance power, SM, and classification at each step of the spectral model optimization.

UV-Vis-NIR	AM1.5G	①BB-pcWLED			②BB-pcWLED+Vis			③BB-pcWLED+Vis+UV			④BB-pcWLED+Vis+UV		
range	(W/m²)	(W/m²)	SM	Class	(W/m²)	SM	Class	(W/m²)	SM	Class	(W/m²)	SM	Class
300-470	139.25	80.354	1.733	C	92.225	1.510	C	138.705	1.004	A+	138.706	1.004	A+
470-561	139.55	130.533	1.069	A+	137.701	1.013	A+	137.767	1.013	A+	137.768	1.013	A+
561-657	138.86	138.584	1.002	A+	134.638	1.031	A+	134.657	1.031	A+	134.658	1.031	A+
657-772	138.67	144.396	0.960	A+	141.192	0.982	A+	141.187	0.982	A+	141.188	0.982	A+
772-919	138.66	146.093	0.949	A+	137.663	1.007	A+	137.624	1.008	A+	146.552	0.946	A+
919-1200	138.96	15.866	8.758	NA	15.192	9.147	NA	15.442	8.999	NA	136.485	1.018	A+
300-1200	**833.94**	655.83			658.61			705.38			**835.36**		

within the Class A+ range, across the wavelength region it covers. In this case, the maximum achievable irradiance was 655.83 W/m² (Table 2, Column 3). This result shows that using a single BB-pcWLED chip can generate an irradiance spectrum that meets Class A+ criteria in four wavelength ranges: 471–561 nm, 561–657 nm, 657–772 nm, and 712–919 nm, where 0.875 < SM < 1.125, according to IEC 60904-9:2020 (see Table 3, Columns 4–5).

An analysis of the SM values reveals that the ranges 471–561 nm (SM = 1.069), 657–772 nm (SM = 0.960), and 712–919 nm (SM = 0.949) deviate somewhat from the ideal AM 1.5G reference spectrum, indicating areas for improvement in subsequent steps. Meanwhile, the wavelength ranges 300–470 nm and 919–1200 nm cannot be covered by the BB-pcWLED alone. These gaps may be addressed by adding UV and NIR LEDs in the final stage. The spectral output designed in this step is illustrated in Figure 2(a).

In the second simulation step, ② BB-pcWLED + Visible LEDs, to reduce spectral deviations in the ranges 471–561 nm, 657–772 nm, and 712–919 nm, the irradiance of the BB-pcWLED was reduced from 655.83 W/m² to 618.47 W/m². Additional visible LEDs with peak wavelengths at 415, 470, 490, and 660 nm were introduced, contributing 7.06, 11.83, 12.09, and 9.17 W/m², respectively (Table 2, Columns 4–5). This adjustment resulted in a total irradiance of 658.61 W/m², while maintaining the spectral distribution within Class A+ across four wavelength ranges: 471–561 nm, 561–657 nm, 657–772 nm, and 712–919 nm. The corresponding SM values were 1.013, 1.031, 0.982, and 1.007, respectively, as shown in Table 3 (Columns 7–8). The spectrum obtained in this step is illustrated in Figure 2(b), showing a clear reduction in spectral deviation. The spectral peaks now align more closely with the AM 1.5G reference spectrum, indicating a significant improvement. However, after this step, the irradiance in the 300–417 nm range remains low, resulting in an SM rating of Class C (Table 3, Column 8). Therefore, the addition of UV spectrum components is required to elevate the SM in this range to Class A+, as will be discussed in the next step.

The third step, ③ BB-pcWLED + Visible + UV LEDs, aims to reduce spectral deviation in the 300–471 nm wavelength range, thereby achieving a SM value close to 1.000. This was accomplished by adding UV LEDs with peak wavelengths at 325, 340, 365, and 385 nm, contributing irradiance values of 8.01, 13.09, 17.21, and 0.45 W/m², respectively (Table 2, Columns 7–8). The total irradiance power achieved in the 300–417 nm range was 138.705 W/m², resulting in an SM of 1.004, which meets the Class A+ criterion (Table 3, Columns 10–11). This means that, according to IEC 60904-9:2020, the resulting simulated spectrum distribution qualifies as Class A+ in five wavelength ranges: 300–417 nm, 471–561 nm, 561–657 nm, 657–772 nm, and 712–919 nm, with SM values of 1.004, 1.013, 1.031, 0.982, and 1.008, respectively (Table 3, Columns 10–11). The spectrum obtained from this step is illustrated in Figure 2(c), showing a clear reduction in spectral deviation. The spectral peaks align closely with the AM 1.5G reference spectrum, demonstrating a strong match across the five ranges.

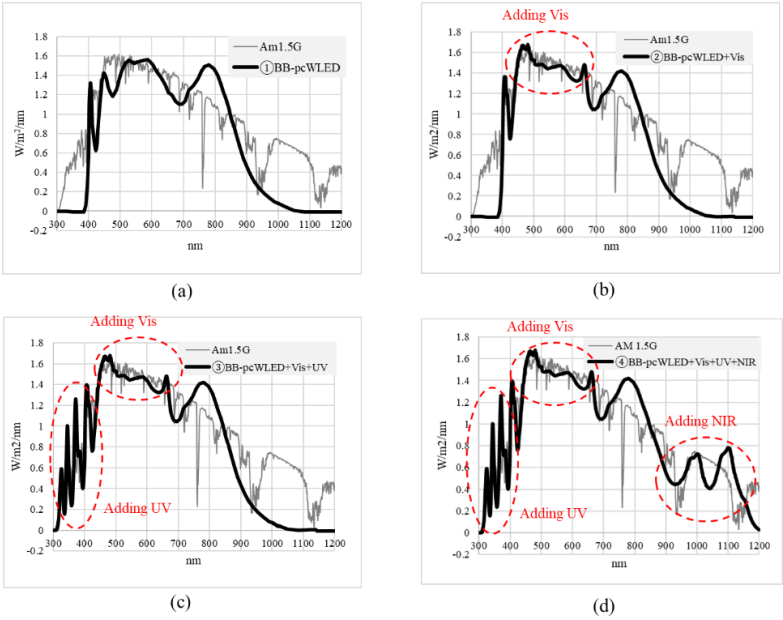

Fig. 2 Simulated spectrum of the BB-pcWLED and step-by-step adjustments during the optimization process.

However, following this step, the irradiance in the 919 - 1200 nm range remains low, at only 15.442 W/m², significantly below the AM 1.5G reference value of 138.96 W/m², a difference of 123.52 W/m². This shortfall prevents the SM in this region from meeting Class A+ requirements. Therefore, in the next step, the addition of NIR spectrum components will be necessary to elevate the SM in this region to Class A+.

The final step, ④ BB-pcWLED+Vis+UV+NIR, addresses the limitations identified in the previous stage. To enhance the spectral performance in the 919 - 1200 nm wavelength range, the author added four NIR LEDs with peak wavelengths at 880, 1,000, 1,100, and 1,150 nm, contributing 5.49, 48.47, 55.27, and 20.75 W/m², respectively (Table 2, Columns 10 - 11). The total irradiance contributed by the NIR LEDs was 129.97 W/m². As a result, the total irradiance in the 919–1,200 nm range increased to 136.485 W/m², yielding an SM of 1.018, which satisfies the Class A+ criteria (Table 3, Columns 13–14).

This indicates that the optimized spectrum simulation model of the LSS achieves spectral mismatch within the range of 0.946 to 1.031 across all wavelength intervals defined in IEC 60904-9:2020, thereby meeting the Class A+ standard. This result confirms that the simulated spectrum closely matches the AM 1.5G reference spectrum, demonstrating excellent spectral conformity. When applied in photovoltaic (PV) testing, such an LSS can provide high-quality illumination, resulting in more accurate measurements of short-circuit current and photocurrent.

The final spectrum, including the NIR adjustments, is illustrated in Figure 2(d). The total irradiance of the spectral model across the 300–1,200 nm wavelength range is 835.36 W/m². In this study, the configuration BB-pcWLED + Visible + UV + NIR is referred to as the "13-LED A+ spectrum."

3.2 Analysis Results of SPC and SPD

Based on the spectral simulation model of the 13-LED A+ spectrum for the LSS, as reported in Section 3.1 (Figure 3a), the author calculated the SPC and SPD and compared the results with LSS spectra from other studies (Figures 3b–3f). These studies were identified through a literature review using the Scopus database, covering the period from 2014 to 2024. The comparison focused on LSS designs with irradiance spectra covering at least the 400 – 1,100 nm wavelength range and achieving Class A of SM, or those spanning the 300-1,200 nm range and meeting Class A+ criteria.

Among the referenced studies, the 6-LED type solar simulator spectrum (Figure 3d) reported in (Vosylius *et al.* 2023) achieved Class A+ performance (Configuration L6) under IEC60904-9:2020, with an SPC of 91.8% and an SPD coverage of 61.1% over the 300-1,200 nm range. Additionally, the author examined solar simulator spectra using more than 13-LED types, including a 14-LED AAA-class solar simulator (Figure 3b) from (López-Fraguas *et al.* 2019), a 15-LED AAA-class simulator (Figure 3c) from (Sun *et al.* 2022), a 19-LED AAA-class LSS (Figure 3e) from (Tavakoli *et al.* 2021), and a 23-LED AAA-class LSS (Figure 3f), previously developed by the author (Linden *et al.* 2014). These models were included in the comparative analysis conducted in this study.

Before analyzing the spectral images from references (Sun *et al.* 2022, Al-Ahmad *et al.* 2022, Tavakoli *et al.* 2021 & Linden *et al.* 2014), the author first converted the spectral images into numerical spectral data using WebPlotDigitizer (Automeris.io. 2025). The extracted data were then calibrated to a wavelength range of 300 to 1,200 nm using the Spectral Mismatch Calculator (PV Lighthouse. 2025), with the Auto Scale Intensity function applied to calibrate their amplitude. Once the spectral data had been calibrated, they were downloaded in spreadsheet format and subsequently used to calculate the SPC and SPD using equations (1) and (2), respectively. The results of the SPC and SPD analysis are summarized in Table 4.

The analysis results from Table 4 indicate that the LED spectral model proposed in this study referred to as the 13-LED A+ spectrum, which combines BB-pcWLEDs (EFFILUX. 2025) with other LEDs (13 types in total) achieved the best performance. It yielded the highest SPC at 99.52%, indicating a spectrum that closely matches natural sunlight, and the lowest SPD at 17.42%, suggesting minimal deviation from the standard AM 1.5G solar spectrum. This demonstrates that the 13-LED A+ configuration provides excellent spectral performance despite using a relatively small number of LED types. In comparison, the study by (Vosylius *et al.* 2023), which utilized only six LED types, also achieved Class A+ status under the new IEC 60904-9:2020 standard (International Electrotechnical Commission. 2020), but resulted in a significantly lower SPC (91.8%) and a much higher SPD (61.1

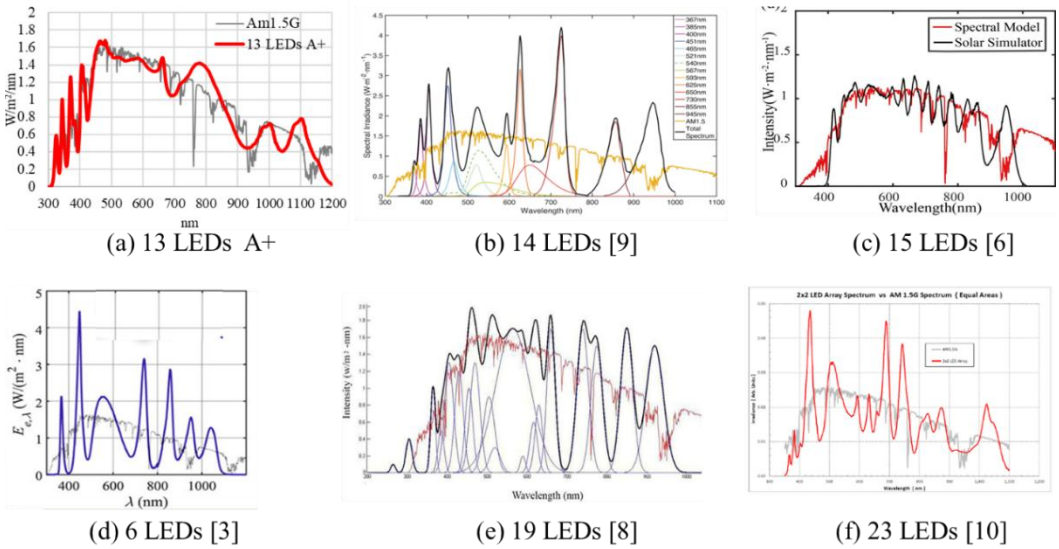

(a) 13 LEDs A+ (b) 14 LEDs [9] (c) 15 LEDs [6]

(d) 6 LEDs [3] (e) 19 LEDs [8] (f) 23 LEDs [10]

Fig. 3 A spectral model of the 13-LED Class A+ LSS compared with the LSS spectra from the references (Vosylius *et al.* 2023, Sun *et al.* 2022, Tavakoli *et al.* 2021, López-Fraguas *et al.* 2019 & Linden *et al.* 2014)

Table 4
Results of the SPC and SPD analysis for all LED spectra used in this study.

Configurations	Spectral Class	Wavelength (nm)	SPC (%)	SPD (%)	References
13 LEDs A+	A+	300 to1,200	**99.52**	**17.42**	Our study
6 LEDs	A+	300 to 1,200	91.80	61.10	(Vosylius *et al.* 2023)
14 LEDs	A	350 to 1,100	61.38	61.07	(López-Fraguas *et al.* 2019)
15 LEDs	A	400 to 1,100	83.32	35.10	(Sun *et al.* 2022)
19 LEDs	A	250 to 1,000	83.94	45.53	(Tavakoli *et al.* 2021)
23 LEDs	A	350 to 1,100	**95.21**	**38.77**	(Linden *et al.* 2014)

%). This indicates a higher deviation from the reference solar spectrum. Even the LSS spectrum from (Linden *et al.* 2014), which incorporated 23 LED types, showed a higher SPD than the 13-LED A+ model proposed in this study.

This comparison highlights that using a larger number of LED types (e.g., 19 or 23) does not necessarily improve spectral performance. For example, the 23-LED configuration achieved a high SPC of 95.21% but still exhibited a relatively high SPD of 38.77%, which is notably higher than that of the 13-LED A+ model. These findings suggest that the selection of LED wavelengths and the optimization of spectral intensity are more critical than the sheer number of LED types used. Moreover, this study confirms that SPC and SPD values do not inherently improve with an increasing number of LEDs. Instead, the performance strongly depends on the type, wavelength, and spectral alignment of the selected LEDs.

However, the LSS spectra reported in (Sun *et al.* 2022, Tavakoli *et al.* 2021, López-Fraguas *et al.* 2019, & Linden *et al.* 2014) were developed under the earlier standard, IEC 60904-9:2007 (International Electrotechnical Commission. 2007), which employed less stringent performance criteria for solar simulators compared to the updated IEC 60904-9-2020 (International Electrotechnical Commission. 2020) For instance, the 2007 standard only required spectral match up to Class A and did not include performance indicators such as SPC and SPD. This aligns with the objective at the time to design and build LSS systems, achieving the best performance under the old criteria, typically classified as Class AAA. As a result, when these spectra are evaluated using the updated 2020 standard, their SPC values tend to be lower, particularly in systems that used fewer types of LEDs. For example, systems using 14 and 15 LEDs yielded SPC values of 61.38% and 83.32% respectively. In contrast, a system using 23 LEDs achieved a higher SPC of 95.21%. These results confirm the earlier design trend: fewer LED types generally led to lower SPC, and increasing the number of LED types improved SPC. However, even with more LED types, the SPD may still not meet the stringent spectral accuracy required by the 2020 standard. This indicates that increasing the number of LED types alone is not sufficient precise wavelength selection and spectral tuning are also essential to meet the new performance metrics.

In summary, based on a comparison with previous studies, the approach proposed in this research using the 13-LED A+ spectrum demonstrates superior performance. The designed spectrum covers the wavelength range from 300 to 1,200 nm, achieving a remarkably high SPC of 99.52%, and the lowest SPD among all compared groups, at 17.42%. These results indicate that the proposed method provides a simulated spectrum closely resembling the standard solar spectrum (AM1.5G), while efficiently utilizing a relatively small number of LED types. Thus, it represents an optimal design for high-performance solar simulation in engineering applications. Moreover, the spectral simulation model developed in this study can serve as a basis for the development of a high-quality prototype LSS in future research.

3.3 Limitations of This Study

The process of generating spectrum data using WebPlotDigitizer may introduce inaccuracies due to several factors, including image resolution, axis calibration errors, and human clicking errors. These potential inaccuracies in the spectral data were not taken into account when calculating the SPC and SPD in Section 3.2 and are acknowledged here as a limitation of the study.

4. Conclusion

The objective of this study was to design and simulation a Class A+ LED Solar Simulator spectrum using BB-pcWLEDs through a data-driven reconstruction approach. This method utilized spectral data from LED manufacturers to identify the minimum number of LED types required to achieve the best SPC and SPD. The results showed that using BB-pcWLEDs (covering 400-900 nm) in combination with UV, visible, and NIR LEDs, 13 types in total, enabled the creation of an irradiance spectrum that meets the Class A+ requirements of IEC 60904-9:2020. The measured SPC and SPD values were 99.52%, and 17.42% respectively, indicating excellent spectral performance. The use of BB-pcWLEDs and the data-driven reconstruction method introduces a new paradigm in LSS spectral design, making it a highly efficient solution for high-end solar simulation in engineering applications. A limitation of this study is the potential inaccuracy of the spectral data derived using WebPlotDigitizer, which may be affected by factors such as image resolution, axis calibration, and manual clicking errors. These deviations could be minimized by using numerical spectral data directly provided by LED manufacturers. This work provides a foundation for future research and development of high-quality LSS systems, applicable in both academic and industrial solar cell testing. The next research direction will focus on developing a hardware prototype of the solar simulator and validating its irradiance spectrum under actual operating conditions, in compliance with IEC 60904-9:2020.

Acknowledgments

The research team sincerely thanks Rajamangala University of Technology Suvarnabhumi for providing the research equipment and laboratory facilities.

Author Contributions: K.W., K.S., C.B., S.C.; Conceptualization, methodology, formal analysis, K.W., K.S. N.W.; writing original draft, N.W., S.C., C.B., W.R.; supervision, resources, K.W., N.W., K.S., C.B.; writing review and editing, validation, K.W., S.C., W.R.; project administration, funding acquisition. All authors have read and agreed to the published version of the manuscript.

Funding: This research was partially funded by Bangkokthonburi University and Rajamangala University of Technology Suvarnabhumi, whose support made this publication possible.

Conflicts of Interest: The authors declare no conflict of interest.

References

Al-Ahmad, A. Y., Clark, D., Holdsworth, J. L., Vaughan, B., Belcher, W. J., & Dastoor, P. C. (2022). An Economic LED Solar Simulator Design, *IEEE Journal of Photovoltaics*, 12(2), 521-525; https://doi.org/10.1109/JPHOTOV.2022.3143460

ASTM International. 2015 ASTM E927-10 (2015). Pennsylvania: ASTM International. Standard Specification for Solar Simulation for Photovoltaic Testing.

Automeris.io. WebPlotDigitizer. https://automeris.io/ accessed on 1 May 2025

Basore, E.T., Wu, H., Xiao, W., Zheng, G., Liu, X. & Qiu, J. (2021) High-power broadband NIR LEDs enabled by highly efcient blue-to-NIR conversion. *Advanced Optical Materials*, 9(7), 2001660, https://doi.org/10.1002/adom.202001660

Chojniak, D., Schachtner, M., Reichmuth, S. K., Bett, A. J., Rauer, M., Hohl-Ebinger, J., Schmid, A., Siefer, G. & Glunz, S. W. (2024). A Precise Method for the Spectral Adjustment of LED and Multi-Light Source Solar Simulators. Progress in Photovoltaics: *Research and Applications*, 32(6) 372–389, https://doi.org/10.1002/pip.3776

Cortés-Severino, R., Cárdenas-Bravo, C., Barraza, R., Sánchez-Squella, A., Lefort, P. V. & Castillo-Burns, F. (2021). Optimal design and experimental test of a solar simulator for solar photovoltaic modules. *Energy Science & Engineering*, 9(2), 2514-2528, https://doi.org/10.1002/ese3.985

Cruz, G. P. C.; Barreto, G. L.; Gómez-Malagón, L. A.; de Lima, R. A.; & Vital, C. V. P. (2025) Solar Simulator Prototype With Halogen and Light-Emitting Diode Sources. *J. Sol. Energy Eng.*, 147(4), 041005, https://doi.org/10.1115/1.4067972

EFFILUX. Hyperspectral lighting systems. https://www.effilux.com/en/products/hyperspectral accessed on 4 May 2025

EPIGAP OSA Photonics. IR LED chips. https://www.epigap-osa.com/led-chips/ir-led-chips/ accessed on 4 May 2025

Esen, V., Sağlam, Ş., & Oral, B. (2017). Light sources of solar simulators for photovoltaic devices: A review. *Renewable and Sustainable Energy Reviews*, 77, 1240-1250. https://doi.org/10.1016/j.rser.2017.03.062

Ge, C., Fang, Q., Lin, H. & Hu, H. (2021). Review on Blue Perovskite Light-Emitting Diodes: Recent Advances and Future Prospects. *Frontiers in Materials*, 8, 635025, https://doi.org/10.3389/fmats.2021.635025

Hasan, M. M., Jones, E., & Rahman, F. (2024). Stable solvatochromic light-emitting diodes and their potential for color temperature adjustment of white LEDs. *Optical Materials*, 152, 115490, https://doi.org/10.1016/j.optmat.2024.115490

Hou, D., Lin, H., Zhang, Y., Lin, Z., Li, H., Song, J., & Huang, R. (2023). A novel extra-broadband visible-NIR phosphor doped with Ce^{3+} and Cr^{3+} towards multifunctional advanced applications. *Ceramics International*, 49(7), 10692-10701; https://doi.org/10.1016/j.ceramint.2022.11.259

International Electrotechnical Commission (2020) *IEC 60904-9: 2020*. Photovoltaic Devices - Part 9: Classification of Solar Simulator Characteristics.

International Electrotechnical Commission. (2007). *IEC 60904-9: 2007*. Photovoltaic Devices - Part 9: Solar simulator performance requirements.

Islam, N. U., Usman, M., Rasheed, S., & Jamil, T. (2021). Review—White Light-Emitting Diodes: Past, Present, and Future. *ECS Journal of Solid State Science and Technology*, 10(10), 106004, https://doi.org/10.1149/2162-8777/ac26d8

Katzin, D., Leo, Marcelis, F.M., & Mourik, S. V. (2021). Energy savings in greenhouses by transition from high-pressure sodium to LED lighting. *Applied Energy*, 281, 116019, https://doi.org/10.1016/j.apenergy.2020.116019

King, P., Merlière, E., Gosteli, C., Coto, I. M., Reed, J., Tucker, M., Karim, M. & Almond, H. (2023). Design of a low-cost high-flux solar simulator. *AIP Conference Proceeding*, 2815, 080003, https://doi.org/10.1063/5.0148835

Leary, G., Switzer, G., Kuntz, G. & Kaiser, T. (2016). Comparison of xenon lamp-based and led-based solar simulators, *IEEE Photovoltaic Specialists Conference (PVSC)*, Portland, OR, US, 21 Nov 2016, 3062–3067, https://doi.org/10.1109/PVSC.2016.7750227

Linden, K. J., Neal, W. R., & Serreze, H. B. (2014). Adjustable spectrum LED solar simulator. *Light-Emitting Diodes: Materials, Devices, and Applications for Solid State Lighting XVIII*, 9003, 109–117; https://doi.org/10.1117/12.2035649

López-Fraguas, E., Sánchez-Pena, J. M., & Vergaz, R. (2019). A Low-Cost LED-Based Solar Simulator, *IEEE Transactions on Instrumentation and Measurement*, 68(12), 4913-4923; https://doi.org/10.1109/TIM.2019.2899513

Marubeni America Corporation. 1150 nm IR LED datasheet (SMT1150D). https://tech-led.com/wp-content/uploads/2021/07/SMT1150D.pdf accessed on 1 May 2025

Parupudi, R. V., Singh, H., & Kolokotroni, M. (2019). Sun Simulator for Indoor Performance assessment of Solar Photovoltaic Cells. *Energy Procedia*, 161, 376-384, https://doi.org/10.1016/j.egypro.2019.02.102

PV Lighthouse. Spectral mismatch calculator. https://www2.pvlighthouse.com.au/calculators/spectral%20mismatch%20calculator/spectral%20mismatch%20calculator.aspx accessed on 5 May 2025

Sena, S., Kumari, S., Kumar, V. & Husen, A. (2024). Light emitting diode (LED) lights for the improvement of plant performance and production: A comprehensive review. *Current Research in Biotechnology*, 7, 100184, https://doi.org/10.1016/j.crbiot.2024.100184

Sevilla-Camacho, P.Y., Robles-Ocampo, J.B., Rodríguez-Resendíz, J., Cruz-Arreola, D. S., Sánchez-Hernández, F. & Solís-Cisneros, H.I. (2024). Evaluation of the design features and components for a large-scale solar simulator for PV module testing, *Solar Energy*, 279, 112836, https://doi.org/10.1016/j.solener.2024.112836

Song, J. Y., Zeng, R. M., Xu, D. Y., Wang, Y., Ding, Z., & Yang, C. (2021). A compact AAA-compatible multispectral solar simulator based on spherical cap chamber. Solar Energy, 220(15), 1053-1064, https://doi.org/10.1016/j.solener.2021.03.074

Sun, C., Jin, Z., Song, Y., Chen, Y., Xiong, D., Lan, K., Huang, Y., & Zhang, M. ((2022). LED-based solar simulator for terrestrial solar spectra and orientations, *Solar Energy*, vol. 233, 96-110; https://doi.org/10.1016/j.solener.2022.01.001

Sun, Y., Shang, M., Wang, Y., Zhu, Y., Xing, X., Dang, P., & Lin, J. (2023). The ultra-wideband near-infrared luminescence properties and applications of $K_2SrGe_8O_{18}:Cr^{3+}$ phosphor. *Ceramics International*, 49, 32619-32627, https://doi.org/10.1016/j.ceramint.2023.07.229

Tavakoli, M., Jahantigh, F., & Zarookian, H. (2021). Adjustable high-power-LED solar simulator with extended spectrum in UV region, *Solar Energy*, 220, 1130-1136; https://doi.org/10.1016/j.solener.2020.05.081

Thorlabs Inc. LEDs for scientific applications. https://www.thorlabs.com/navigation.cfm?guide_id=2101 accessed on 1 May 2025

Turek, M., Sporleder, K. & Luka, T. (2019). Spectral characterization of solar cells and modules using LED-based solar simulators, *Solar Energy Materials and Solar Cells*, 194, 142-147, https://doi.org/10.1016/j.solmat.2019.02.007

Vosylius, Ž., Antonovič, D., Novičkovas, A., Gaubas, E., & Tamošiūnas, V. (2023). Rational selection of light sources for LED-based solar simulators. *Solar Energy*, 265, 112064. https://doi.org/10.1016/j.solener.2023.112064

Vosylius, Ž., Novičkovas, A., & Tamošiūnas, V. (2023). Optimization of LED-Based Solar Simulators for Cadmium Telluride and Microcrystalline Silicon Solar Cells. *Energies*, 16(15), 5741; https://doi.org/10.3390/en16155741

Vosylius, Ž., Novičkovas, A., Laurinavičius, K. & Tamošiūnas, V. (2022). Rational Design of Scalable Solar Simulators With Arrays of Light-Emitting Diodes and Double Reflectors. *IEEE Journal of Photovoltaics*, 12(2), 512-520, https://doi.org/10.1109/JPHOTOV.2021.3136783

Wang, C.; Wang, X.; Zhou, Y.; Zhang, S.; Li, C.; Hu, D.; Xu, L.; Jiao, H. (2019). An Ultra-Broadband Near-Infrared Cr^{3+}-Activated Gallogermanate $Mg_3Ga_2GeO_8$ Phosphor as Light Sources for Food Analysis. *ACS Applied Electronic Materials*, 1(6), 1046-1053, https://doi.org/10.1021/acsaelm.9b00219

Wang, X., Feng, X., Molokeev, M. S., Zheng, H., Wang, Q., Xu, C., & Li, J. G. (2023). Modulation of Bi^{3+} luminescence from broadband green to broadband deep red in Lu_2WO_6 by Gd^{3+} doping and its applications in high color rendering index white LED and near-infrared LED. *Dalton Transactions*, 52(9), 2619-2630; https://doi.org/10.1039/D2DT03751C

Watjanatepin, N., Boonmee, C., Kaisookkanatorn, P., Sritanauthaikorn, P., Wannakam, K., & Thongkullaphat, S. (2023). Light Sources and Irradiance Spectrum of LED solar simulator for photovoltaic devices: A Review. *International Journal of Renewable Energy Research (IJRER)*, 13(1), 192-207. https://doi.org/10.20508/ijrer.v13i1.13741.g8675

Watjanatepin, N., Wannakam, K., Kiatsookkanatorn, P., Boonmee, C., & Sritanauthaikorn, P. (2023). Improved spectral mismatch and performance of a phosphorconverted light-emitting diode solar simulator. *International Journal of Electrical & Computer Engineering(IJECE)*, 13(5), 4931-4941; http://doi.org/10.11591/ijece.v13i5.pp4931-4941

Yang, J., Zhang, G., Zhao, B., Yang, D., Zhang, K., Zhang, Y., Zhang, J., Ren, Z., Sun, J., Wang, L., Mo, X., Ren, T., Ren, D., Peng, Z., Yang, S., & Lv, J. (2025). Solar Spectrum Simulation Algorithms Considering AM0G and AM1.5G. *Sensors*, 25(5), 1406, https://doi.org/10.3390/s25051406

Zhang, J., Fang, L., Wu, H., Zhang, L., Wu, H., Pan, G., & Zhang, J. (2024). Ce^{3+} and Cr^{3+} co-activated ultra-wide visible-NIR garnet phosphor for phosphor-converted light emitting diode. *Materials Research Bulletin*, 177, 112870; https://doi.org/10.1016/j.materresbull.2024.112870